NORSAR

ROYAL NORWEGIAN COUNCIL FOR SCIENTIFIC AND INDUSTRIAL RESEARCH

Scientific Report No. 2-79/80

SEMIANNUAL TECHNICAL SUMMARY 1 October 1979—31 March 1980

By
A. Kr. Nilsen (ed.)

Kjeller, June 1980

VI. SUMMARY OF TECHNICAL REPORTS/PAPERS PREPARED

VI.1 An Experimental Small Subarray within the NORSAR array: Crustal Phase Velocities and Azimuths from Local and Regional Events

In October 1979, NORSAR subarray 06C was modified to a small aperture array - NORESS - with station distances in the range 125 - 2051 m. Fig. VI.1.1 gives the former and present configuration of 06C. All six sensors are now equipped with 8 Hz lowpass filters.

The purpose of the NORESS experiment is to obtain data from closely spaced sensors in order to

- Investigate noise and signal coherencies at high frequencies
- Identify P, S and Lg phases from regional seismic events
- Detect and locate regional events.

The first two items above are the subject of this contribution.

Fig. VI.1.2 shows a map of seismic events in Fennoscandia that occurred during the first half year of operation of the experimental array. These events are located by the regional seismic network with typical location uncertainties of 10-30 km.

Both signal and noise coherencies have been evaluated for the 'new' array. An example of how the records of NORESS compare with those of an ordinary subarray at NORSAR is given in Fig. VI.1.3. For this Lg phase the waveform changes rather drastically from sensor to sensor within a 'normal' NORSAR subarray (6 top traces from subarray 02B) with a diameter about 10 km and typical sensor spacings of 3-4 km. The NORESS array proves to offer a significant improvement in this respect, as can be seen from the lower 6 traces. The epicentral distance is the same for the two subarrays.

For both signal and noise, coherencies are given in Figs. VI.1.4 and VI.1.5 for 2 and 4 Hz, respectively, for all station combinations within NORESS. The noise data set consists of 20 blocks each of 512 samples of 20 Hz data, amounting to a total of 8.53 minutes. This time interval was carefully selected to avoid detectable signals within it. The signal is a 12 seconds interval (1 block of 240 samples), of an Lg phase for

an event about 200 km away and in appearance very similar to the one in Fig. VI.1.3. Fig. VI.1.5 shows that coherency at 4 Hz is maintained at a level above 0.5 out to about 1 km and then drops to a random level. This point should serve to illustrate the need for small station separations in the study of regional Lg waves. For lower signal frequencies the coherency is maintained at a relatively high level throughout the range of NORESS station distances.

For the processing of NORESS data the high-resolution frequency-wavenumber analysis has been applied to all distinct phases for the events in Fig. VI.1.2. The single frequency theoretical response pattern of the NORESS array is shown in Fig. VI.1.6. For slow phases (phase velocity in the order of 3.5-4.0 km s^{-1}) and high frequencies (say 5 Hz), the corresponding wavenumber is larger than 1 km^{-1} and side lobe effects due to array response might become important. On the other hand, P phases of all frequencies (8 Hz lowpass filters aplied to all channels) should have a fair chance of being correctly determined by such an array.

Fig. VI.1.7 shows records from the 6 NORESS sensors for event no. 1 (earthquake) in Fig. VI.1.2. For each of the phases P_n, P and Lg in this figure, high-resolution frequency-wavenumber plots were produced for 5 different frequencies and all for 100 samples (5 sec) of each phase. For the P_n phase the results are shown for three frequencies in Fig. VI.1.8. According to the reporting agency (UPP), the 'true' azimuth from NORESS to the epicenter is 104^o, while the three frequencies displayed give values of 98^o, 97^o and 103^o. All wavenumber grids consist of 31 x 31 points, yielding an azimuth resolution of about $3\text{-}4^o$ for this phase. The phase velocity values fluctuate around 8 km s^{-1} but could not be attributed to anything else than a P phase of some kind. In the following analysis, for each phase analyzed we will select the frequency or equivalently the azimuth and phase velocity corresponding to the largest power. For the Lg phase of the same event, the corresponding results are given in Fig. VI.1.9. The analysis of this phase serves to illustrate the side lobe problems encountered in a few cases. The frequency (3.5 Hz) corresponding to the largest power gives a maximum power in k-space which obviously results from spatial aliasing and the azimuth

and phase velocity values are thus misleading. The other 4 frequencies analyzed, like 4.5 Hz (shown in Fig. VI.1.9) give, however, 'correct' values both for phase velocity and azimuth.

Event 2 of Fig. VI.1.2 is a mining blast at Titania Gruber, Hauge i Dalane. The NORESS records in Fig. VI.1.10 show only one clear phase (Lg), while the P phase is hardly detectable by eye. However, a 5-sec interval including the expected P-arrival time is processed with the result given in Fig. VI.1.11 for the frequency corresponding to the largest power. The analogous result for the Lg phase is also given in Fig. VI.1.11. The 'true' azimuth in this case is 233^{o}, i.e., the Lg and P results are both 'wrong' by about 10^{o}.

With the exception of a few cases for which spatial aliasing effects are easily identified, all phase velocities are plotted in Fig. VI.1.12 for the events in Fig. VI.1.2. All measurements correspond to the one frequency out of five that has the maximum power. With the k-space grid that has been used, the phase velocity resolution is typically 0.3-0.4 km s^{-1}. Where more than one P phase is available, only the strongest (in terms of power) is included in this figure. On the basis of this figure, the following conclusions are readily reached.

- The P and Lg phases separate into nonintersecting phase velocity bands and a discrimination between P and Lg is possible from NORESS data.
- It is hardly possible to separate Lg from S (the S phases here are believed to be S_n) on the basis of phase velocity measurements alone.

The evaluation of the NORESS array continues and will include the following items:

- Processing of new events as they become available.
- Alteration of the array geometry to remove all side lobes from the part of the k-space corresponding to $|k| < 2$ km^{-1} to eliminate all spatial aliasing problems.
- Do high-resolution frequency-wavenumber analysis with a denser grid in wavenumber space for more detailed phase velocities.

S. Mykkeltveit, F. Ringdal & H. Bungum

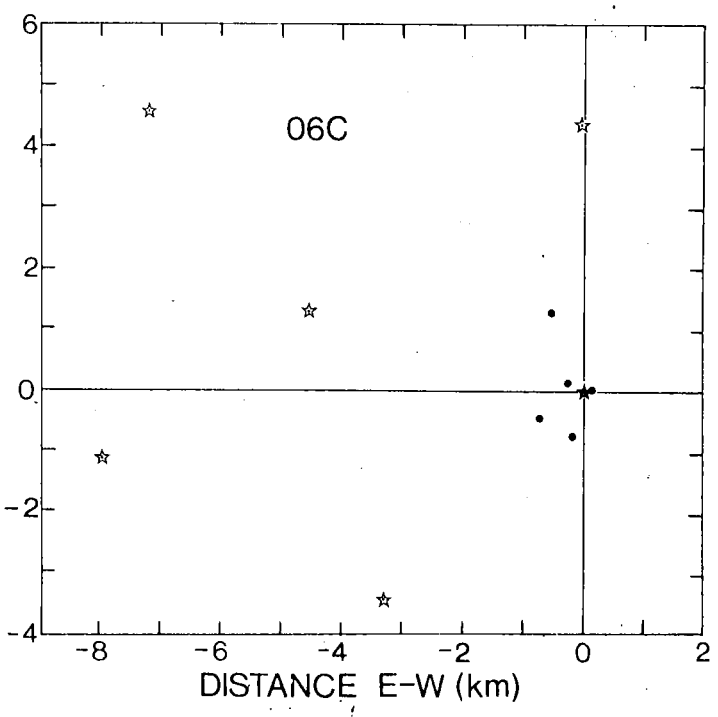

Fig. VI.1.1 Geometry of the 06C subarray before (stars) and after (dots) the change in October 1979. NORESS location is given by the star.

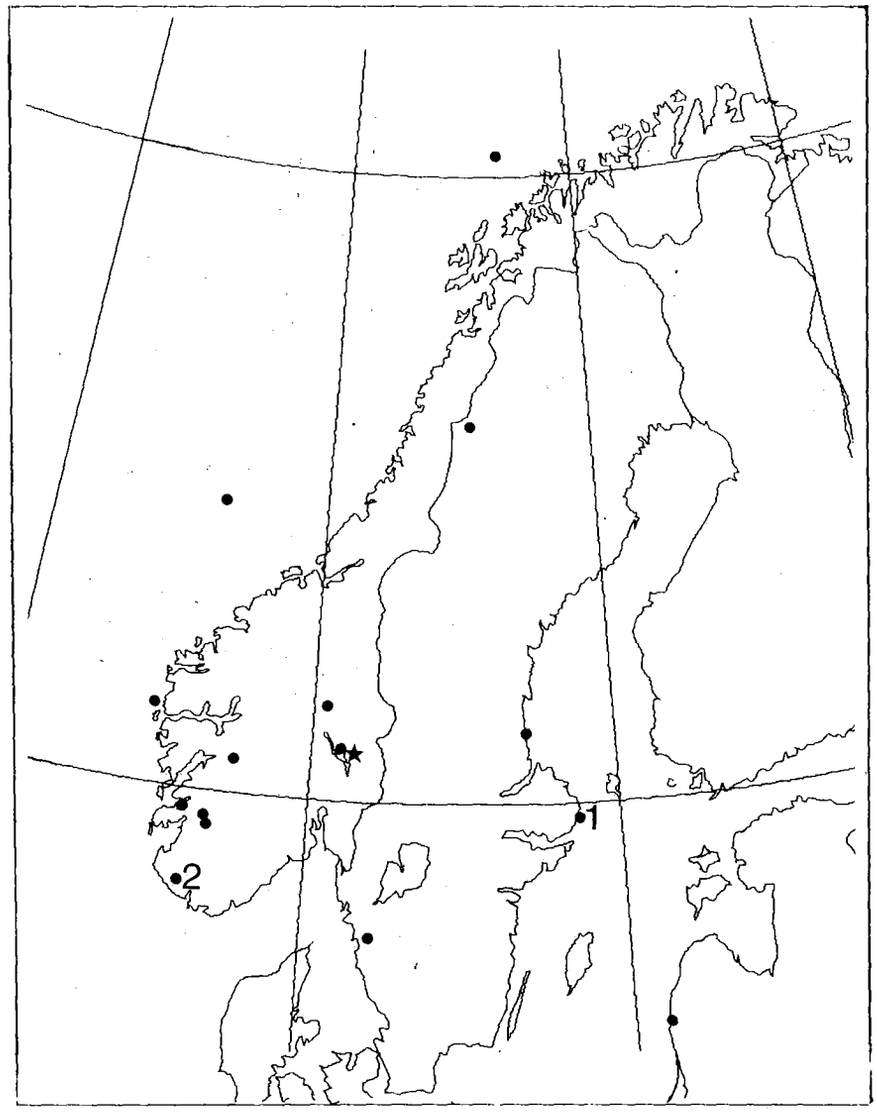

Fig. VI.1.2 Seismic events in Fennoscandia for the period October 1979-April 1980 as located by various agencies on the basis of the regional station network.

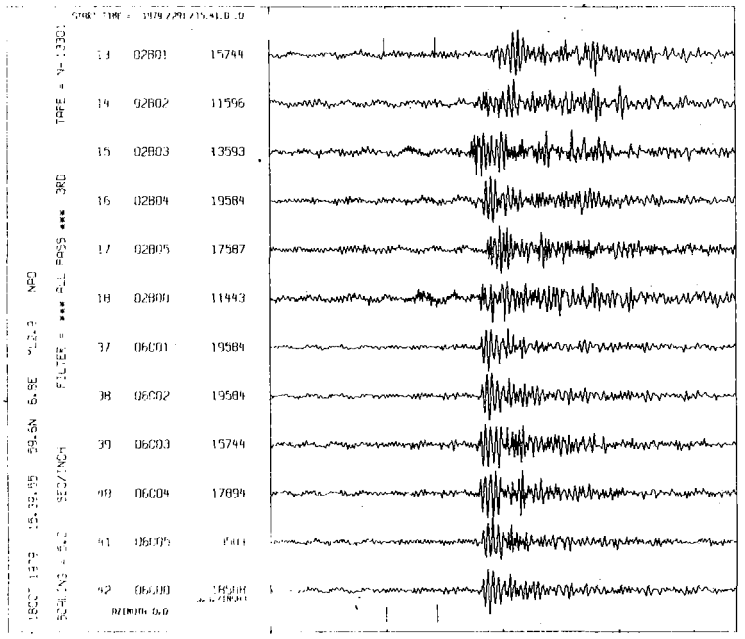

Fig. VI.1.3 Lg waves from an explosion about 300 km away. The top six traces are from standard subarray 02B, the lower six traces from NORESS. The time interval covered is 40 sec.

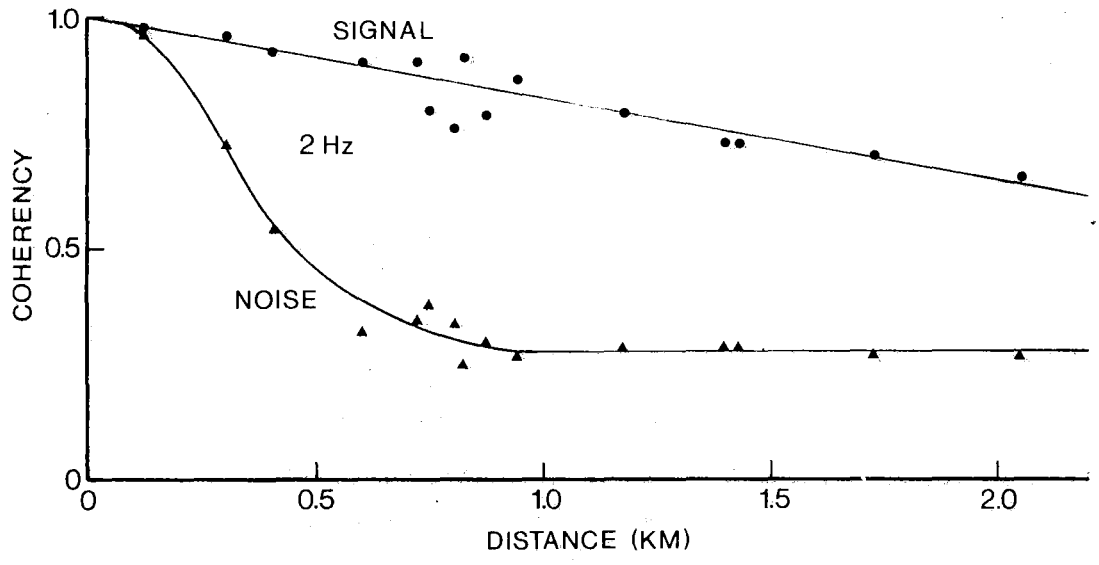

Fig. VI.1.4 Signal and noise coherencies at 2 Hz as a function of sensor distances within NORESS.

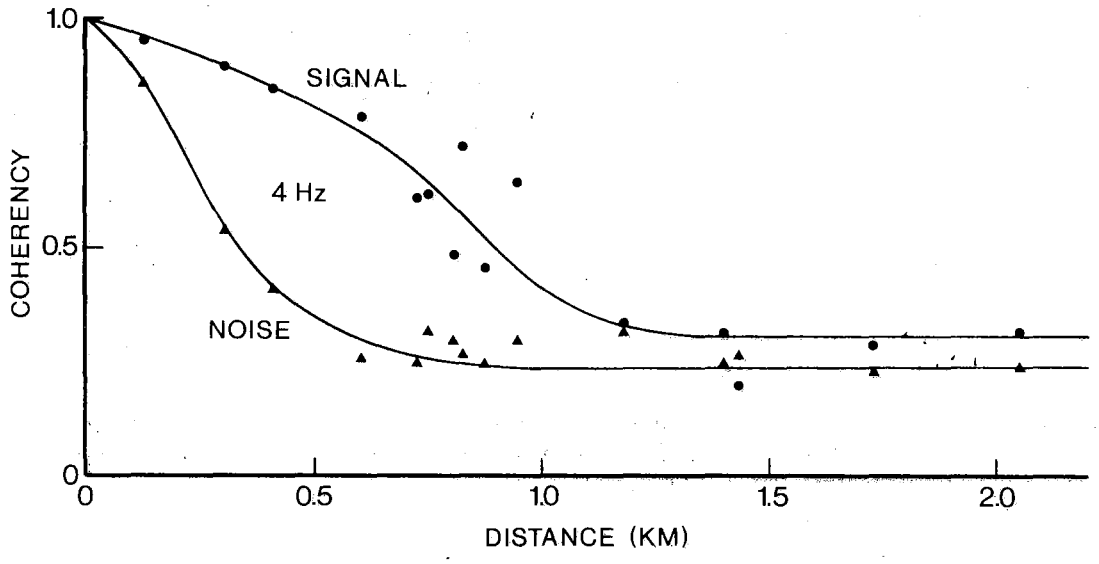

Fig. VI.1.5 Same as Fig. VI.1.4, for 4 Hz.

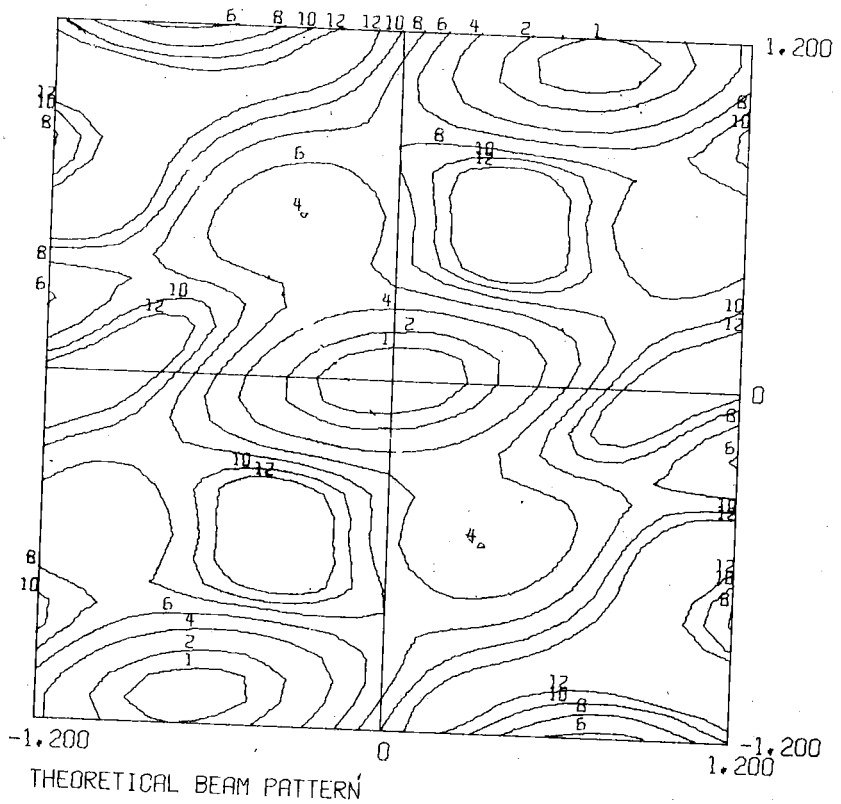

Fig. VI.1.6 Single frequency theoretical response pattern for NORESS.

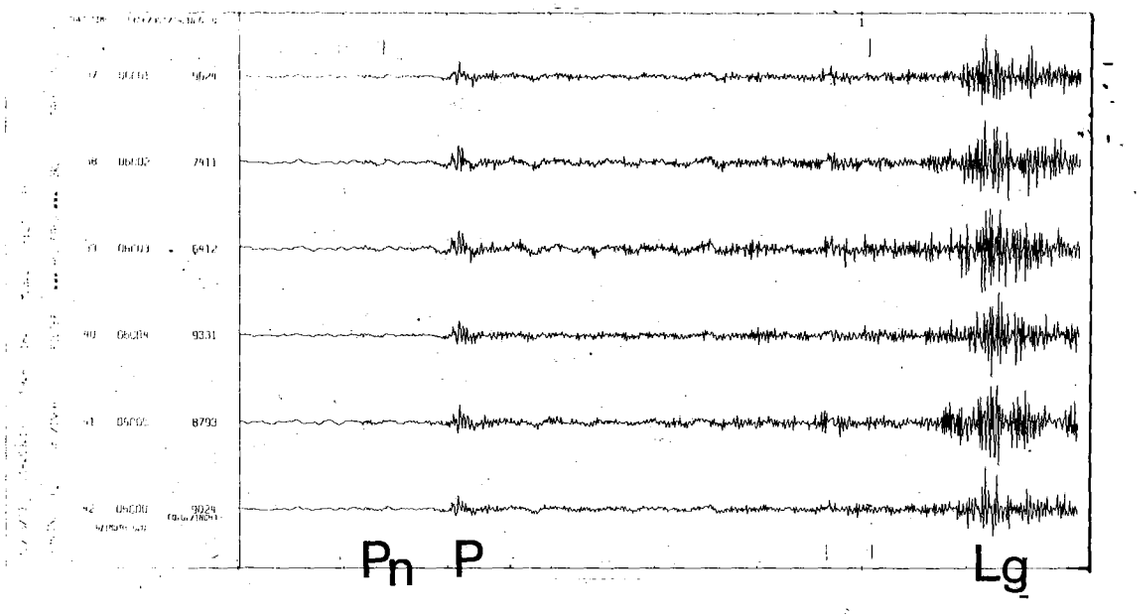

Fig. VI.1.7 NORESS records for event 1 in Fig. VI.1.2. The epicenter information is as reported by Uppsala. The time window covers 80 sec.

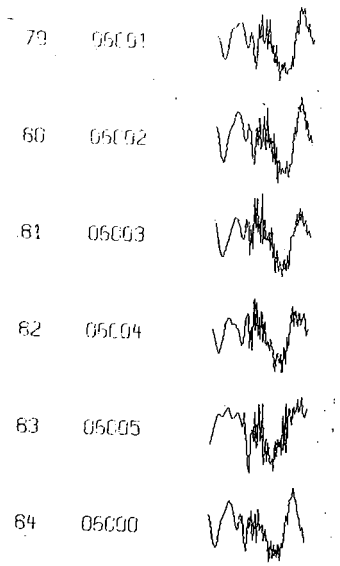

P_n

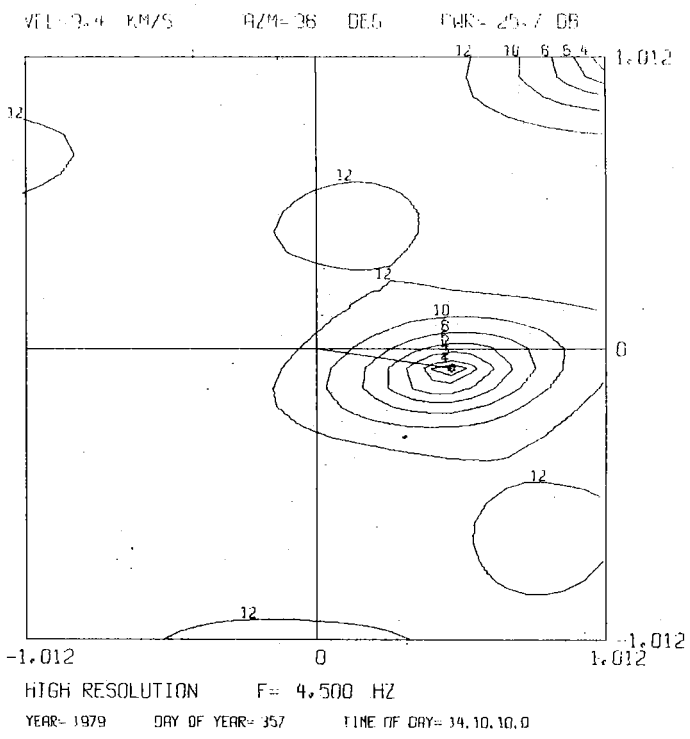

P_n

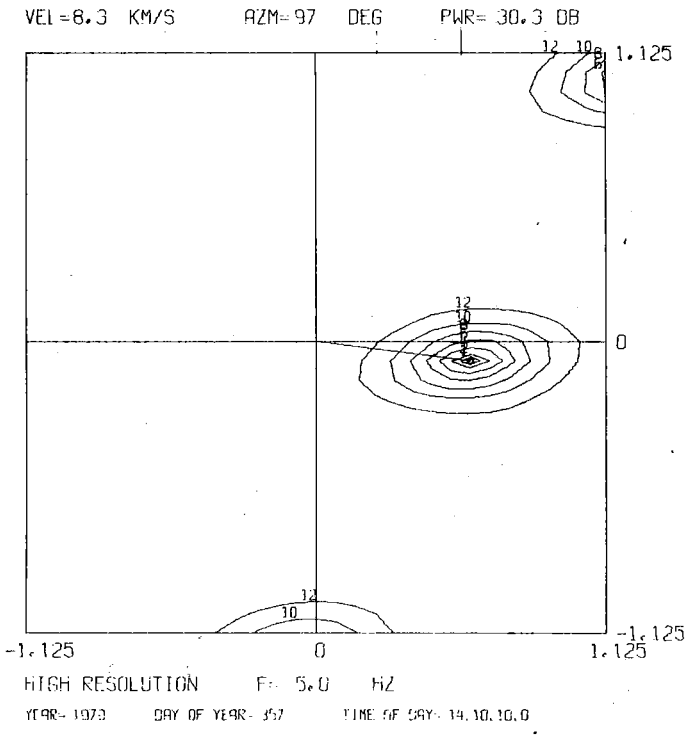

P_n

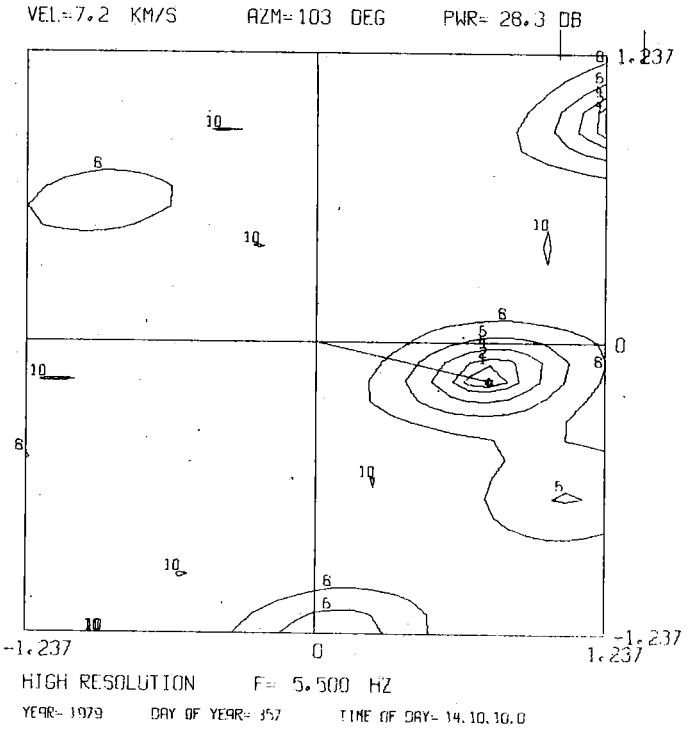

P_n

Fig. VI.1.8 High-resolution frequency-wavenumber plots at three frequencies for the 5 sec of the P_n phase shown in upper left corner.

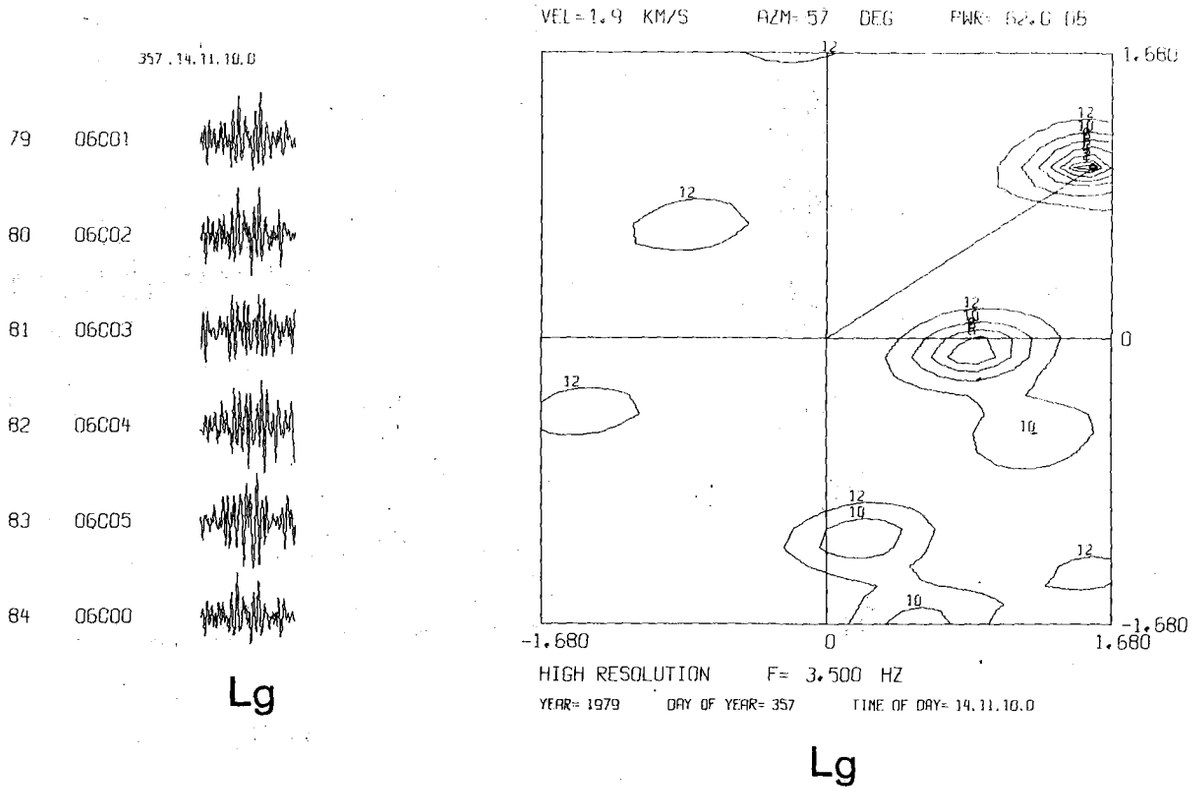

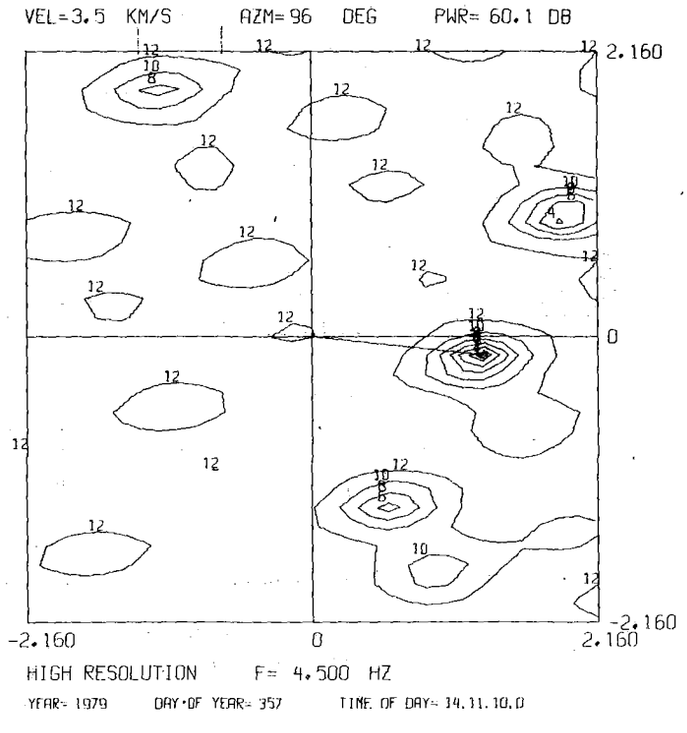

Fig. VI.1.9 Same as Fig. VI.1.8 for two frequencies for the Lg phse.

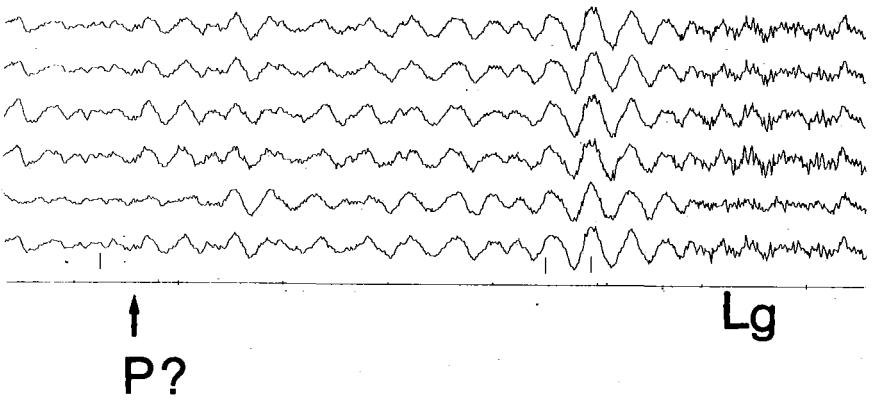

Fig. VI.1.10 NORESS records for event 2 in Fig. VI.1.2 (explosion at Titania Gruber). The time window covers 80 sec.

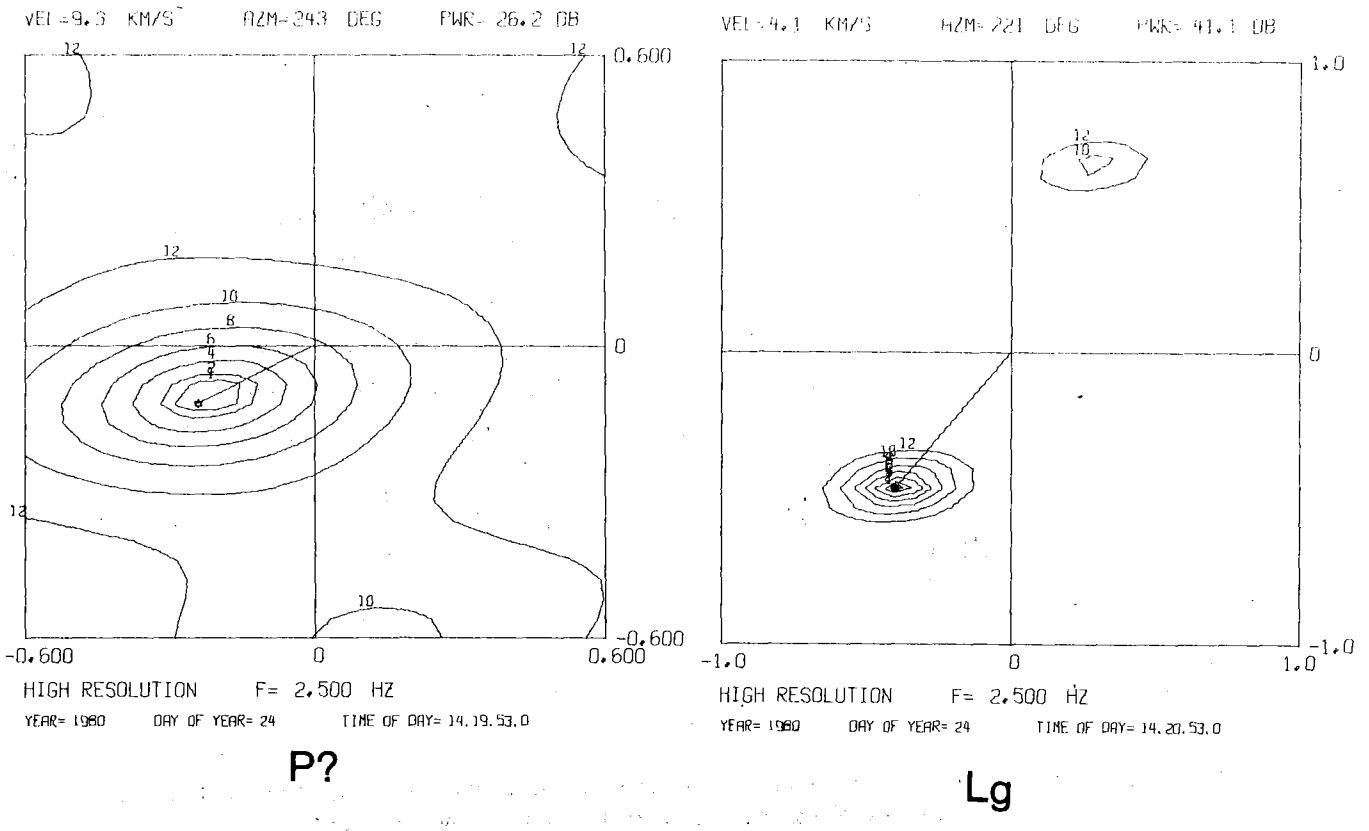

Fig. VI.1.11 High-resolution frequency-wavenumber plots for the P and Lg phases (5 sec of each) from event 2 in Fig. VI.1.2.

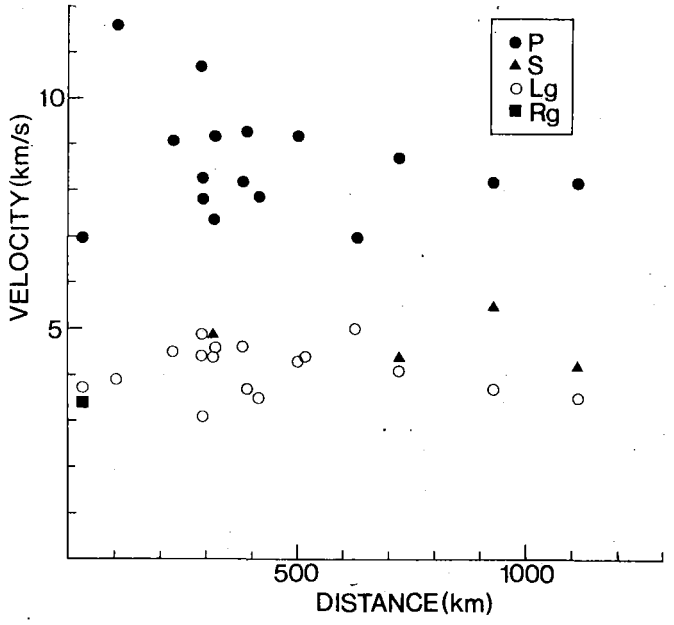

Fig. VI.1.12 Phase velocities as determined by processing of NORESS data from the events of Fig. VI.1.2.